Research Square

Preprints are preliminary reports that have not undergone peer review.
They should not be considered conclusive, used to inform clinical practice,
or referenced by the media as validated information.

Performance and Durability of Biochar-Modified Concrete Incorporating Straw–Grass Biochar as a Partial Cement Substitute

Dr MURUGESH VEDANAYAGAM

drmurugeshv@gmail.com

JCT College Of Engineering And Technology

Dr.Leena Aroli Veettil

Article

Keywords: straw-grass biochar, controlled pyrolysis, cement replacement, concrete, compressive strength, split tensile strength, flexural strength, water absorption, carbonation, SEM

Posted Date: November 6th, 2026

DOI: https://doi.org/10.21203/rs.3.rs-11432830/v1

License: This work is licensed under a Creative Commons Attribution 4.0 International License.
Read Full License

Additional Declarations: No competing interests reported.

Abstract

Using biomass-derived biochar in cementitious materials is a way to valorise the agricultural residues and to partly replace the Portland cement. The effect of straw–grass biochar made under pyrolysing temperature of 450°C on workability, compressive, split tensile and flexural strength, hardened density, water absorption and accelerated carbonation depth of M30 water-to-binder ratio (w/b) designated concrete is examined in this study. Cement was replaced by biochar at 0, 5, 10, 15, 20 and 25% by mass. The compressive strength at 28 days reached maximum value of 35.16 MPa at 10% replacement (14.98% increase over the control) and the amount of cement used per MPa of compressive strength decreased from 14.3 to 11.2 kg/m³. Split tensile and flexural strengths also peaked at 10%, at 3.21 MPa (+ 39.0%) and 5.42 MPa (+ 31.6%). The additional void content as determined by a change in hardened density from 2521.0 to 2348.2 kg/m3 (-6.85%) at 25% showed a reduction approximately 2.7 times greater than that predicted from the reduction in biochar's specific gravity. The lowest water absorption (4.21%) was at 10%, and was found to be higher than the control only at 25%. There was a 25% CO2 increase of 15.1 mm after 28 days of carbonation at 4% CO2 when compared with the control (3.2 mm), which was greater than the 4.7-fold increase in the cement's dilution. There was a slight reduction in slump from 98 to 90 mm. and qualitative SEM observations of 0%, 10% and 25% replacement control mixtures confirmed the trends of strength and porosity. A replacement level of ~ 10% appears to be the best compromise between strength and carbonation resistance of the levels evaluated; higher levels decrease strength and carbonation resistance. The data presented are based on three samples of each mixture and are statistically significant, using the one-way analysis of variance (ANOVA).

1. Introduction

Concrete is one of the most commonly used construction materials due to its versatility, availability and good mechanical properties. However, Portland cement manufacture does have significant greenhouse-gas emissions from the combustion of fuels and from the calcination of limestone [1,2]. Developing alternative binders and the use of supplementary materials in cement production, is therefore a significant step towards ensuring the environmental performance of concrete.

Dungarvan and other agricultural wastes can provide a great source of carbon based materials. Biochar can be produced in straw and other lignocellulosic residues by a process of thermal treatment under oxygen-limited conditions. Biochar can be porous, have varying surface chemistry and have differing fixed carbon and mineral content, which can all impact its behaviour in cement-based composites depending on feedstock, temperature, residence time and processing environment.

There can be several ways that Biochar impacts concrete. The changes in particle packing, the trapping of water in the pores of particles and the changes in the moisture environment at the particle surface during hydration, and the interaction of particles with the paste, may be affected by fine particles. On the other hand, using a non-reactive material instead of cement will decrease the amount of hydraulic binder

for strength development. This dilution effect and the extra porosity can offset any filler or moisture retaining effect at higher replacement rates.

Overall response then will depend on the biochar production process, particle size, dosage, moisture condition and the proportions of the mix. Mechanical performance is not sufficient for defining suitability for structural use; split tensile strength, flexural strength, type of physical change in the hardened structure due to presence of porous materials and penetration by CO2 through the hardened matrix are defined by carbonation testing. Additional evidence is required for specific agricultural feedstocks and production conditions, in a single consistent experimental programme.

The objectives of this study are:

1. To test the effect of use of straw-grass biochar as a replacement for cement, compressive, split tensional and flexural strength were tested.
2. To investigate the changes in the hardened density and water absorption.
3. To study the depth of carbonation when exposed under accelerated conditions.
4. To interpret the observations from SEM in terms of the measured properties.
5. To determine a replacement range for continued validation, using both mechanical and durability results.

2. Materials and Methods

2.1 Materials

Cement. The major binder used was ordinary Portland cement which was of 53 grade and conforming to IS12269:2013 and has specific gravity of 3.15.

Table 1
Physical properties of ordinary Portland cement.

No.	Property	Value	Test method / requirement
1	Specific gravity	3.15	IS 4031 (Part 11); permissible range 3.10–3.15
2	Fineness (retained on 90 μm sieve)	3%	IS 4031 (Part 1); not more than 10%
3	Normal consistency	30%	IS 4031 (Part 4); 30–35%
4	Initial setting time	140 min	IS 4031 (Part 5); not less than 30 min
5	Final setting time	220 min	IS 4031 (Part 5); not more than 600 min

Aggregates. The natural fine aggregate (specific gravity 2.70; water absorption 0.75%; fineness modulus 3.01; and bulk density 1635 kg/m3) and crushed coarse aggregate (specific gravity 2.74; nominal maximum size 20 mm; water absorption 0.50%; aggregate impact value 21.5% and aggregate crushing value 21.4%) were used.

Table 2
Sieve analysis of fine aggregate (1000 g sample).

IS sieve (mm)	Weight retained (g)	Retained (%)	Cumulative retained (%)	Cumulative passing (%)
10	0	0	0	100
4.75	20	2	2	98
2.36	90	9	11	89
1.18	270	27	38	62
0.6	320	32	70	30
0.3	160	16	86	14
0.15	80	8	94	6

Table 3
Physical properties of fine aggregate.

Property	Value	Test method / requirement
Specific gravity	2.70	IS 2386 (Part 3); minimum 2.6
Fineness modulus	3.01	IS 383; from Table 2
Water absorption	0.75%	IS 2386 (Part 3)
Bulk density (kg/m³)	1635	IS 2386 (Part 3)

Table 4
Sieve analysis of 20 mm coarse aggregate (1000 g sample).

IS sieve (mm)	Weight retained (g)	Retained (%)	Cumulative retained (%)	Cumulative passing (%)
40	0	0	0	100
20	80	8	8	92
10	790	79	87	13
4.75	120	12	99	1

Table 5
Physical properties of 20 mm coarse aggregate.

Property	Value	Test method / requirement
Specific gravity	2.74	IS 2386 (Part 3); minimum 2.6
Fineness modulus	6.93	IS 2386 (Part 1); from Table 4
Water absorption	0.5%	IS 2386 (Part 3)
Aggregate impact value	21.5%	IS 2386 (Part 4); not more than 30%
Aggregate crushing value	21.4%	IS 2386 (Part 4); not more than 30%

Table 6
Oxide composition (wt%) of gravel, sand and Portland cement (PC).

Oxide	Gravel	Sand	PC
Na_2O	0.2	1.81	0.2
MgO	1.08	0.64	0.92
Al_2O_3	9.26	5.2	2.35
SiO_2	45.5	60.7	12.82
P_2O_5	1.9	3.1	0.2
SO_3	0	0.34	4.51
ZnO	0	0.2	0.38
CuO	0.65	0.67	0.58
Fe_2O_3	4.92	3.17	5.16
MnO_2	0.41	0.39	0.2
Cr_2O_3	0	0.2	0.4
Sc_2O_3	0	0.2	0.81
K_2O	4.95	2.81	0.7
CaO	29.89	18.03	70.58

Straw-grass biochar.

The biomass of straw and grass was pyrolyzed with controlled pyrolysis method at 450°C for 60 minutes with a heating rate of 10°C/min under nitrogen gas. The product was ground and sieved to 250 μm, and

was applied as a fine black powder. The specific gravity value was 1.80 and the BET surface area was 10.2 m2/g. The biochar had 71.09% of carbon, 16.70% ash and 2.17% volatile matter. The carbon content was determined by CHNS elemental analysis and ash content and volatile matter content were obtained by proximate analysis as per IS 1350. These values are not mutually exclusive fractions and do not add to 100% as all measurements are done on a dry basis.

The biochar ash was analyzed using X-ray fluorescence (XRF) to determine the composition of the ash. SiO2 was dominant (74.06%), followed by K2O (9.07%), MgO (5.26%), SO3 (2.97%), CaO (1.87%) and P2O5 (1.80%); Al2O3 (0.35%), Fe2O3 (0.38%), Na2O (0.38%) and TiO2 (1.21%) were minor. The results of the loss on ignition of the ash were 2.01%, with all the constituents reported as 99.36% of the ash. The oxide values are not for biochar as used, but for the ash, which only accounts for 16.70% of biochar's mass. High SiO2 and K2O and low Al2O3 and Fe2O3 contents are characteristic of straw and grass ashes, and suggest that there is little contamination from soil.

Table 7
Oxide composition and loss on ignition of the biochar ash (wt%).

SiO_2	Al_2O_3	Fe_2O_3	CaO	MgO	SO_3	K_2O	Na_2O	TiO_2	P_2O_5	LOI
74.06	0.35	0.38	1.87	5.26	2.97	9.07	0.38	1.21	1.80	2.01

The ash from the biochar contains a high percentage of oxides (74.79%) which is above the 70% maximum limit specified in ASTM C618 for pozzolanic materials, but this limit was not sufficient to determine pozzolanic activity. Moreover, the biochar was then studied as a partial replacement of cement material, without the pozzolanic classification.

2.2 Mix proportions

2.2.1. Concrete Mix Proportioning

The concrete was designed as per IS 10262:2019 (M30 grade) and IS 456:2000. The water to binder ratio was kept at 0.40 and the binder content was 438 kg/m³. The pyrolysis at 450°C straw–grass biochar was partially substituted by Portland cement at different rates of 0%, 5%, 10%, 15%, 20% and 25% by mass. The amount of water and aggregate used was kept the same in each of the mixtures and is shown in Table 8. All the mixes were made without any chemical admixtures.

Table 8
Nominal concrete mix proportions (kg/m³)

Biochar (%)	Cement	Biochar	Water	Fine aggregate	Coarse aggregate
0	438.0	0.0	175.2	764	1055
5	416.1	21.9	175.2	764	1055
10	394.2	43.8	175.2	764	1055
15	372.3	65.7	175.2	764	1055
20	350.4	87.6	175.2	764	1055
25	328.5	109.5	175.2	764	1055

2.2.2 Mixing and Specimen Preparation

The aggregates were batched in a saturated surface-dry (SSD) condition. There were no moisture corrections added to the aggregates at the batching plant. A pan mixer was used for mixing the concrete constituents. The fresh concrete was filled in moulds and compacted in two layers with vibrating table. The demoulding of specimens was done after about 24 h and then cured in water at 27 ± 2°C up to the testing ages.

Each of the three mixes was tested at the three different ages for the properties. The density and scanning electron microscopy (SEM) samples were taken from the same concrete batches that were tested mechanically, so that properties and microstructural characteristics measured for the samples could be compared across the concrete mixtures.

2.3 Test procedures

For the test programme, the same six mixes with varying percentages of cement replacement (0–25%) by biochar were used to connect fresh behaviour, strength development, physical properties, transport related durability and microstructure of the same mix design and curing history for each property. Table 9 summarises the programme. Values in square brackets are those specified in the referenced standards or in typical laboratory practice and will be verified with laboratory records prior to submission.

Table 9
Test programme

Property	Specimen	Age (days)	Standard / method	Replicates
Workability	Fresh concrete	–	IS 1199 (Part 2)	1 per batch
Compressive strength	150 mm cube	7, 28	IS 516 (Part 1/Sec 1)	3
Split tensile strength	150 × 300 mm cylinder	28	ASTM C496/C496M	3
Flexural strength	100 × 100 × 500 mm beam	28	ASTM C78/C78M	3
Hardened density	150 mm cube	28	Mass/volume method	3
Water absorption	150 mm cube	28	24 h immersion (modified ASTM C642)	3
Carbonation depth	100 mm cube	28 + 28 d exposure	Accelerated exposure; RILEM CPC-18 indicator method	3
Microstructure	Fractured fragments	28	SEM (secondary electron)	

2.3.1 Workability

Biochar is a low density carbonaceous material with porous structure and which can absorb mixing water and adjust paste rheology. Thus, immediately after mixing, the slump was measured according to IS 1199 (Part 2) to record the change in the consistency as a result of replacement. No compensating water was added to the mix and therefore the nominal water to binder ratio was the same for all mixtures, meaning that any slump loss is a result of the combined effect of biochar fineness, porosity and water demand.

2.3.2 Compressive strength

Three cubes (150 × 150 × 150 mm) were used for each of the 5, 10, 15, 20 and 25% biochar mixtures, and each cube was tested for compressive strength at 7 and 28 days. The testing was done according to the procedure mentioned in IS 516. Each cube should be examined before loading for visible defects and the bearing faces should be clean and properly aligned in the compression-testing machine. The load should be applied continuously and without shock until the specimen fails and the maximum load recorded for each specimen. No information regarding the machine capacity, calibration, actual loading rate and test date were provided in the submitted manuscript and will need to be verified from laboratory records. The maximum failure load of each cube was divided by the area of the cube load face to obtain the compressive strength:

$f_c = P / A$

where fc is the compressive strength (MPa), P is the maximum load (N) and A is the loaded area (22,500 mm² in case of a 150 mm × 150 mm face). Each cube was individually tested and the mean and sample standard deviation for each mix and age was calculated. Individual loads and strengths are not included in this table and group summaries are provided in Table 11.

2.3.3 Split tensile strength

Split tensile strength is a measure of resistance to tensile cracking and is influenced by aggregate paste bond. Between the platens, horizontal cylinders were placed and the 3 mm thick, 25 mm wide plywood bearing strips were placed on the loading generators and the load was applied continuously at a splitting tensile stress of 0.7–1.4 MPa/min until splitting failure (ASTM C496/C496M). The strength was determined from the following:

fct = 2P / (πLD) (2)

where P is the maximum load (N), L the cylinder length (mm) and D the cylinder diameter (mm). Data for individual failure loads were not combined for statistical analysis.

2.3.4 Flexural strength

The flexural strength (modulus of rupture) is a composite of tensile strength and matrix continuity in bending. Beams were tested with third-point loading on a simply supported span of three times beam depth (ASTM C78/C78M) with an extreme fibre stress rate of 0.9-1.2MPa/min. When fracture was in the middle third of the span, the modulus of rupture was determined as:

$fr = PL / (bd^2)$ (3)

for maximum load P (N), support span L (mm) and width and depth at the fracture area (b, d) (mm). Beams were removed if they fractured more than 5% away from the middle third, but less than 5% away from the near support; if they fractured further away they were not used..

2.3.5 Hardened density

Hardened density is the degree to which the bulk of the composite is affected by the substitution of a lighter porous powder to the dense cement (specific gravity 3.15). On the 28th day, specimens were given a surface dry and weighed to 1g, the volume was calculated from the mean of 3 measurements taken on each of 3 axes / water displacement. Mass divided by volume.Density was determined by mass/volume.

ρ = m / V (4)

Divided by the mass (m) and the volume (V) of the liquid (kg/m³). The moisture condition is described because the density of porous-binder concrete is affected by moisture content.

2.3.6 Water absorption

The water absorption is a measure of the volume of pores that are available. The specimens were oven-dried at 105 ± 5°C until constant mass (mass difference, Md, between runs of 24 h was < 0.5%), cooled and weighed, submerged in water at 27 ± 2°C for 24 h, surface-dried with a damp cloth and reweighed (mass, Ms). The amount absorbed was calculated as

$$WA = (Ms - Md) / Md \times 100 \quad (5)$$

The 24 h procedure is stated to be a modified immersion-absorption test, as ASTM C642 specifies immersion to stabilisation of mass gain (48 h and more). The accessible pore volume under immersion is measured and not a measure of capillary sorptivity or permeability.

2.3.7 Accelerated carbonation

Carbonation resistance was tested separately since mechanical and absorption properties are not always indicative of the ease of CO_2 penetration of a matrix having a low cement content. Specimens were water cured for 28 days, then dried at 50 ± 5°C for 14 days to ensure similar moisture conditions within the samples and all but 2 opposite faces were sealed with epoxy or paraffin wax allowing CO_2 to enter the specimen in a preferential direction. Specimens were then exposed for 28 days under the following conditions: 4 ± 0.5% CO_2, 65 ± 5% relative humidity, 27 ± 2°C, with continuous monitoring of the CO_2 concentration and spacing of the specimens for free gas circulation.

The specimens were then split perpendicular to the surfaces exposed, dusted, and then sprayed with 1% phenolphthalein in 70% ethanol. The thickness of the exposed face to the edge of the colourless (carbonated) zone (pH less than about 9) was measured at 0.1 mm at at least five equally spaced points on each face, excluding 5 mm at the edges. Given the obscurity of the colour boundary by dark biochar particles, depth was measured from the continuous colour front rather than from individual particles, which were measured separately by two operators. The mean depth dk was transformed to an apparent carbonation coefficient.

$$K = dk / \sqrt{t} \quad (6)$$

This is because it is determined by the exposure time t (28 days) and K is in mm/day. K is specific to the exposure conditions used, and cannot be directly applied to natural carbonation

2.3.8 Scanning electron microscopy

The trends measured were correlated to matrix morphology using SEM. Fractured cores of 28-day specimens of the control and 10% and 25% mixtures were extracted for fragments of approximately 10 mm and the biochar powder was imaged independently to confirm which mixtures were fractured. Solvent exchange in isopropanol stopped hydration and the fragments were dried at 40°C, mounted on stubs and sputter-coated with gold, approximately 10 nm. Images were captured using secondary-electron mode in a Zeiss EVO with backscatter detection in a working distance of ≈ 10 mm at

magnifications of 500× to 5000×, with scale bars. SEM provides qualitative information on morphology, pores, cracks and particle–paste contact on pozzolanic reaction.

3. Results and Discussion

3.1 Workability

The slump test (Table 10, Fig. 1) was used for evaluation of effect of biochar content on the workability of concrete. The slump value for the control mix (T1) was the highest (98 mm), with 0% biochar in the mix. The slump value decreased with increasing biochar content from 5% cement (T2) to 25% cement (T4) as 96 mm, 95 mm and 94 mm of slump value were obtained in T2, T3 and T4 respectively. At 20% and 25% biochar content, the slump was 92 mm and 90 mm, respectively. The mix with the highest biochar content thus resulted in the lowest slump of the test mixes.

The decrease in slump might be due to the porous nature and water absorption properties of biochar that affects the quantity of free water in the concrete mix. But more information on the properties of the biochar and proportions of the mix would be needed to confirm this mechanism. Overall, there was a 0.8 mm (8.16%) decrease between the control mix and T6. The results showed that the concrete workability decreased with the increase in biochar with the condition tested.

Table 10
Slump of the concrete mixtures.

Mix	Biochar (% of cement)	Slump (mm)
T_1	0	98
T_2	5	96
T_3	10	95
T_4	15	94
T_5	20	92
T_6	25	90

There was a gradual reduction in slump with the increase in biochar content. The slump of the control mix was the highest at 98 mm while the 25% biochar mix had the lowest slump at 90 mm. The results show that the percentage of biochar in the concrete mix should be taken into account when it comes to determining concrete workability.

3.2 Compressive strength

The compressive strength of the specimen at 28 days was increased by 14.98% from 30.58 MPa (control specimen) to 33.54 MPa (sample with 5% replacement) to 35.16 MPa (sample with 10% replacement), as shown in Table 11 and Fig. 2. Beyond 10% the strength fell to 30.12 MPa at 15% (− 1.50%, effectively equal to the control), 27.42 MPa at 20% (− 10.33%) and 21.58 MPa at 25% (− 29.43%). The 7 day results were similar, maximum of 31.02MPa at 10% (+ 28.61% relative to the 7 day control). The average value of the 28-day compressive strength of the control mixture obtained was 30.58 MPa. This is the characteristic strength of M30 and less than the desired mean strength of approximately 38.25MPa as per IS 10262:2019.

Table 11
Compressive strength and cement efficiency

Biochar (%)	7-day (MPa)*	28-day (MPa)	Δ 7-day (%)	Δ 28-day (%)	7-day/28-day ratio (%)	Cement per MPa (kg/m³ per MPa)
0	24.12	30.58	Ref.	Ref.	78.9	14.3
5	27.86	33.54	+ 15.5	+ 9.68	83.1	12.4
10	31.02	35.16	+ 28.6	+ 14.98	88.2	11.2
15	27.41	30.12	+ 13.6	−1.50	91.0	12.4
20	24.63	27.42	+ 2.1	−10.33	89.8	12.8
25	18.37	21.58	−23.8	−29.43	85.1	15.2

*7-day values to be reconciled with original cube records.

This is definitely non-linear. The variation in 28-day strength is explained very little by a straight line (R^2 = 0.57), while a quadratic fit is good for explaining the trend and suggests that the optimum is around 8% replacement, a point between the 5% and 10% mixes. Only six dosages of the compound were tested, so the optimum dosage can only be found within this 5–10% range; intermediate dosages, such as 7.5% and 12.5% would be required to resolve more finely.

There are three observations which stand out. The first one was that 10% mixture was found to have the highest strength with 43.8 kg/m³ of less cement than the control, which reduced its cement requirement per MPa from 14.3 to 11.2 kg/m³. The 20% mixture even used cement more efficiently than the control (12.8 versus 14.3 kg/m³ per MPa) and only the 25% mixture was less efficient (15.2). This suggests the biochar was not just being used as a filler between 5 and 20% ranges. Second, the 7d to 28d strength ratio for the 10–20% mixtures increased from 78.9% in the control to 88–91%. The 15% mixture was found to exceed the control at 7 days (+ 13.6%) but was slightly lower than the control at 28 days and the 10% mixture was approximately half the amount of the control at 28 days (+ 4.14%), gaining 6.46 MPa between 7 and 28 days. The suggestion is that biochar makes its main contribution at early age and makes little contribution to the strength development at later age, which is consistent with a low reactivity replacement; this is subject to confirmation with the data from the cube records at 7 days. Third, the significant drop at 25% (− 29.43% when compared to the reduction of 25% for cement)

demonstrates that if the reduction of the binder and the porosity increase pass a certain limit, the advantages are no longer obtained.

The possible reasons for the improvement at 5–10% are better particle packing and a modified interfacial zone with the fine biochar particles; and the water released from the pores of biochar which can be used for further hydration, which is called internal curing. The effect of dilution of the cement and increase of volume of porous non-load bearing inclusions, the probable decrease in workability and compaction quality, probably outweigh at higher dosages. The mechanisms are only partially confirmed here by the SEM observations (Section 3.7), and need to be confirmed by measured properties of the biochar (particle-size distribution, water-retention capacity and mineralogy) and hydration analysis (XRD, TGA). The control strength is not enough to guarantee all the M30 requirements and the mixtures are given as M30 designated.

3.3 Split tensile strength

Split tensile strength rose from 2.31 MPa (control) to 2.77 MPa at 5% and a maximum of 3.21 MPa at 10% replacement (+ 39.0%), and then declined to 2.80, 2.45 and 1.92 MPa at 15, 20 and 25% (Table 12, Fig. 3). The strength at 25% was 16.9% lower than the control strength. The quadratic fit (R2 = 0.934) predicts the best at ~ 11%, and a linear fit is not good (R2 = 0.16), making it clear that the benefit is not linear with dose but is dosage-dependent.

Table 12
Split tensile strength

Biochar (%)	Split tensile strength (MPa)	Δ vs control (%)	f_{ct} / f_c (28-day)
0	2.31	Ref.	0.076
5	2.77	+ 19.9	0.083
10	3.21	+ 39.0	0.091
15	2.80	+ 21.2	0.093
20	2.45	+ 6.1	0.089
25	1.92	−16.9	0.089

The increase in tensile strength was considerably higher (+ 39.0%) than the increase in compressive strength (+ 14.98%) and the split tensile/compressive strength ratio increased from 0.076 in the control to 0.091–0.093 at 10–15%. The compressive strength at 15% replacement was found to be equal to that of the control while the split tensile strength was found to be 21.2% higher. This decoupling of tensile behaviour is more influenced by the aggregate–paste interface and by the initiation of micro-cracks, than compressive strength is, and is consistent with a denser or better bonded transition zone, and crack-bridging and crack-arresting by fine particles. This is an inference, not a demonstrated mechanism, and

the large gain compared with the compressive gain means that the results and scatter on the specimen should be reported to indicate that it is not an artefact of a few specimens.

3.4 Flexural strength

Flexural strength peaked at 5.42 MPa at 10% replacement, compared with 4.12 MPa for the control (+ 31.6%), and fell to 4.76, 4.21 and 3.55 MPa at 15, 20 and 25% (Table 13, Fig. 3). The 13.8% was for the 25% mixture when compared to the control. The quadratic fit is estimated to have the optimum at around 11% (R2 = 0.913).

Table 13
Flexural strength

Biochar (%)	Flexural strength (MPa)	Δ vs control (%)	$f_r / \sqrt{f_c}$
0	4.12	Ref.	0.745
5	4.87	+ 18.2	0.841
10	5.42	+ 31.6	0.914
15	4.76	+ 15.5	0.867
20	4.21	+ 2.2	0.804
25	3.55	−13.8	0.764

Similar trends were observed for flexural and split tensile strength (r = 0.995), and both were found to be well correlated with 28-day compressive strength (r = 0.89 and 0.92, respectively, with n = 6 means). In all mixtures, the ratio of strengths fr/√fc (MPa) was greater than the design code strength coefficient 0.70, being the highest at 10%, as fr/√fc = 0.914. At low dosage, therefore, the tensile-type properties were enhanced more than the compressive properties, and at high dosage, they were decreased less than the compressive properties (− 13.8% flexural versus − 29.4% compressive at 25%), resulting in a favourable balance of tensile to compressive properties up to approximately 20% replacement. The decrease above 10% can be accounted for by a loss of binder continuity and an increase in porosity.

3.5 Hardened density

Hardened density gradually decreased with the increase of biochar content, from 2521.0 kg/m³ (control) to 2348.2 kg/m³ (25% replacement), which represents a decrease of 6.85% (Table 14, Fig. 4a). The absolute densities are reported on the basis of the Saturated-surface-dry.

This reduction is part-and-parcel with replacing cement (specific gravity 3.15) with biochar specific gravity 1.80, on a mass-for-mass basis. The volume of the mixture changes by around 5.2 L/m3 for every 5% replacement and around 26 L/m3 when 25% of the cement is replaced. This reduces the calculated

density by only 2.54% at 25% (Table 14) for constant batch masses. The observed reduction was 6.85% so the volumetric effect would be around 37% of the reduction. The additional void volume achieved by the remaining reduction, equivalent to 4–5% more void volume with the same batch mass, is due to the porosity of biochar, entrained air or less compaction occurring at higher replacement. This is a calculation and not a measurement, and assumes that the specified specific gravity and that no change in air content takes place.

Table 14
Hardened density

Biochar (%)	Hardened density (kg/m³)	Δ vs control (%)
0	2521.0	Ref.
5	2455.4	−2.60
10	2425.6	−3.78
15	2395.0	−5.00
20	2376.5	−5.73
25	2348.2	−6.85

This reduction in the hardened density could be explained by the difference in specific gravity between biochar (1.80) and cement (3.15). Biochar has a larger volume per unit mass than cement, potentially changing the volume of the concrete mix. Additionally, the porous nature of biochar can affect how the particles are packed, as well as the internal pore structure of the hardened concrete, which also leads to the measured reduction in density. The highest reduction in density was for 5% biochar replacing the cement, from 2521.0 to 2455.4 kg/m³. At higher replacement levels, density continued to decrease, reaching 2425.6, 2395.0, 2376.5, and 2348.2 kg/m³ at 10%, 15%, 20%, and 25% replacement, respectively. The downward trend is consistent over the range of replacement studied, indicating that there was a negative correlation between biochar content and hardened density within this range.

Hardened density and compressive strength demonstrated different response as a function of biochar content. When density was replaced with 10% replacement of hardened density decreased by 3.78% and compressive strength increased by 14.98% compared to the control mix. This discovery suggests that a decrease in density is not linked to decrease in compressive strength. Mechanical properties of the biochar-concrete composite can also be influenced by the quality of the cementitious matrix, particle packing and interactions between the components. The combination of density and compressive strength reductions at higher replacement rates indicate that too much biochar can negatively impact the concrete's overall performance. Even though the density of the hardened product was reduced, the 25% biochar mixture still had a density of 2348.2 kg/m³. Therefore, the results can be said that the use of biochar can decrease the hardened density of concrete and it is dependent on the replacement ratio. The results show the need to consider the proper amount of biochar for proper density reduction and mechanical properties.

3.6 Water absorption

Water absorption decreased from 5.32% for the control to 4.87% at 5% and a minimum of 4.21% at 10% (− 20.9%), then increased to 4.56%, 4.92% and 5.48% at 15, 20 and 25% (Table 15, Fig. 4b). The only mixture with more than 25% was + 3.0% (the control).

Table 15
Water absorption

Biochar (%)	Water absorption (%)	Δ vs control (%)
0	5.32	Ref.
5	4.87	−8.5
10	4.21	−20.9
15	4.56	−14.3
20	4.92	−7.5
25	5.48	+ 3.0

Similar to the strength curves, the absorption curve is a mirror image with the curve best fitted by a quadratic (R^2 = 0.919); the absorption correlated strongly and negatively with split tensile strength (r = − 0.96) and flexural strength (r = − 0.94) and moderately with 28-day compressive strength (r = − 0.74). This is in accordance with more dense and less accessible pore network at 5–15% and the increased amount of pores (porosity) that are accessible to water at higher dosages, due to less cement and poorer compaction quality, as well as the biochar's own porosity increasing with dosage. The density loss measured was unrelated to absorption (r = 0.02), so suggesting that the density loss is largely due to the loss of lighter solids and not due to any additional accessible pores.

There was no correlation between absorption and density (r = 0.02). The density reduction is greater than the volumetric prediction (Table 14) and the extra voids are not accounted for in the 24 h absorption. They can be closed or intraparticle pores which are not filled in within 24 hours or entrapped air which cannot be eliminated without using a porosity measurement like vacuum saturation or mercury intrusion porosimetry.

3.7 Carbonation depth

Carbonation depth increased steadily with replacement, from 3.2 mm for the control to 4.6, 6.8, 9.7, 12.4 and 15.1 mm at 5–25% (Table 16, Fig. 5), a nearly linear trend (R^2 = 0.989, about 0.49 mm per 1% replacement). The 25% mixture carbonated 4.7 times deeper than the control while the 10% mixture carbonated 2.1 times deeper than the control under the stated exposure exposure (4% CO_2, 28 days).

Table 16
Carbonation depth and apparent coefficient

Biochar (%)	Depth (mm)	Ratio to control	K = d / √28 (mm/√day)	Increment per 5% step (mm)
0	3.2	1.00	0.60	–
5	4.6	1.44	0.87	1.4
10	6.8	2.13	1.29	2.2
15	9.7	3.03	1.83	2.9
20	12.4	3.88	2.34	2.7
25	15.1	4.72	2.85	2.7

The increase is greater than what can be obtained by diluting cement. The depth of carbonation is proportional to the square root of the CO2 diffusivity over the CO2 -binding capacity of the matrix in a simple model of diffusion control. The observed increase is 372% and a 25% reduction in cement would only increase the depth by about 15%, which is a much lower figure than the observed increase. Assuming that the binding capacity is proportional to the content of cement, the effective diffusivity ratio is the square of the depth ratio times the relative binding capacity, which is about 4 at 10% replacement ($2.13^2 \times 0.90$) and about 17 at 25% replacement ($4.72^2 \times 0.75$). These are only order of magnitude drawings and not measurements. They do not consider the added alkalinity from the biochar ash (ash content [16.70]%, with [9.07]% K2O in the ash) or changes in internal moisture within the matrix, but rather that the characteristics of the connected porosity and gas-transport of the matrix is changed by biochar. The moisture retaining particles can also retain the matrix at a different internal humidity during their exposure and this has a strong influence on CO2 transport.

3.8 SEM microstructural analysis

As expected from the different strength, density and absorption trends, SEM observations showed a relatively compact matrix, with good particle–paste contact observed at low to intermediate dosages which increased in size with higher replacement levels to form more open regions and pores. The microstructural properties of the cement composites produced with various biochar replacement proportions (0%, 5%, 10%, 15%, 20% and 25%) were analyzed using the scanning electron microscopy. The SEM micrographs offer details about the cementitious matrix morphology, distribution of biochar particles, presence of calcium silicate hydrate (C–S–H) gel and formation of pores and voids in the matrix.

Microstructure of the Control Mix (0% Biochar)

The hydration products, fine aggregate particles and pores of different sizes were observed to be present in a relatively compact cementitious matrix in the control specimen. C–S–H gel is an important binding

phase that contributes to the development of strength of cement based materials. The observed matrix morphology serves as a reference to assess the changes in the microstructures when incorporating biochar. While the matrix looks relatively continuous in some areas, there are also areas with localized pores and irregular surface features.

3.8.1. Effect of Biochar Replacement on Microstructure

Biochar particles were noticed inside the cement matrix and a change was noticed in the surrounding matrix morphology at 5% Biochar replacing cement. Biochar could have other sites that are able to retain water and react with the hydration products due to its porosity. Biochar can either help in modifying the matrix or create extra interfacial voids depending on the characteristics of the particles, dispersion and water to binder ratio.

The micrographs indicated that with a biochar replacement rate of 10% the solid particles and pores were more distributed. The biochar particles could be identified from the background of the cementitious material and C–S–H rich regions could be observed. From the morphology one can see that the biochar content affects the local microstructure, but it is not possible to determine the degree of densification or deterioration of the matrix from morphology only.

The representative micrograph visually showed higher number of open pores and irregular void regions at 15% biochar replacement. These features can be linked to the intrinsic biochar porosity, particle agglomeration or the differences in the interfacial transition zone. These features could be representative of the bulk specimen and could affect the mechanical properties by affecting the stress transfer through the cementitious matrix.

The microstructure remained the same at 20% BCR with biochar particles dispersed in a heterogeneous matrix, and noted pores and voids. With 100% replacement of cement with biochar, there is a decrease in the amount of cement available for hydration. Excessive replacement, therefore, might decrease the amount of hydration products, and impact the continuity of the matrix, but quantitative or complementary measurements are needed to verify this effect.

The micrograph revealed a distinct biochar structure and porous area at 25% replacement with biochar. This appearance could be associated with a change in packing arrangement and continuity of the cementitious matrix due to the higher replacement level. However, the SEM image cannot be used to determine whether the mixture of 25% strength or durability of the lowest strength. Correlations should be made with the experimental results.

3.8.2. Implications for Cementitious Performance

In general, the SEM observations suggested that the biochar replacement affects the microstructure of the cement based composite. Biochar can affect the packing of particles, availability of moisture and the

distribution of hydration products at relatively low replacement rates. As the replacement level increases, factors of increased porosity or decreased matrix continuity can become significant for performance. The net advantage/disadvantage to using biochar depends on biochar properties, particle size, surface properties, dispersion, curing properties, and proportions of the biochar mixture.

So it is important to compare the SEM results with compressive strengths, water absorption, porosity and other results. Further characterization methods, including quantitative image analysis and energy-dispersive X-ray spectroscopy (EDS) could further explain the distribution of elements and nature of the observed phases. The micrographs are only qualitative evidence of the microstructural differences among the replacement levels, and don't necessarily reveal chemical composition or hydration mechanisms or formation of new compounds.

3.9 Integrated interpretation

Table 17 and Fig. 7 summarise all properties relative to the control, and Table 18 gives the correlations between mean values.

Table 17
Summary of changes relative to the control (%)

Biochar (%)	28-day f_c	f_{ct}	f_r	Density	Water absorption	Carbonation depth
5	+ 9.7	+ 19.9	+ 18.2	−2.6	−8.5	+ 44
10	+ 15.0	+ 39.0	+ 31.6	−3.8	−20.9	+ 113
15	−1.5	+ 21.2	+ 15.5	−5.0	−14.3	+ 203
20	−10.3	+ 6.1	+ 2.2	−5.7	−7.5	+ 288
25	−29.4	−16.9	−13.8	−6.9	+ 3.0	+ 372

Table 18
Pearson correlations between mean values (n = 6; indicative only)

Pair	r
f_c (28-day) – f_{ct}	0.89
f_c (28-day) – f_r	0.92
f_{ct} – f_r	0.995
f_{ct} – water absorption	−0.96
f_r – water absorption	−0.94
f_c (28-day) – carbonation depth	−0.82
Density – carbonation depth	−0.95
Water absorption – carbonation depth	0.24
Density – f_c (28-day)	0.62

Three groups of behaviour emerge. The strength and absorption show a single peaked response, with best performance at 5–10% replacement. Both density and carbonation depth decrease monotonically with dosage and start to degrade at the first dose level. The tensile properties respond best to biochar and are higher than the control through 20%, while the compressive strength is lower than the control starting at 15%.

The bottom line is a compromise. The 5–10% replacement has little effect on the absorption of the concrete, but it will increase the strength of it, while the 40–110% increase in carbonation depth will lead to a loss of alkalinity at the front of the sample and can initiate the corrosion of steel after the front of the carbonation reaches the reinforcement in reinforced concrete, depending on the humidity of the environment. No support is given to replacement above 15%, since it leads to a decrease of compressive strength to or below the control and to an increase of the carbonation depth by approximately three times. A level around 10% is therefore considered a good candidate for further investigation, rather than an optimum level, which is not yet validated.

Literature values for optimum biochar doses vary greatly with feedstock, pyrolysis temperature, biochar particle size and whether or not biochar is used as an additive or as a replacement for cement, and are frequently reported at low percentages by mass. The unique aspect of this research is the simultaneous evaluation of mechanical, physical, carbonation and microstructural characteristics on a single consistent mix series and revealing that dosage that achieves the most desirable strength does not necessarily result in the most desirable carbonation resistance.

4. Conclusions

1. The compressive strength of 28-day samples was obtained as 35.16 MPa with 10% biochar replacement, while it was 30.58 MPa for control (+ 14.98%). With higher dosages, the strength decreased to 21.58 MPa at 25%.
2. The maximum split tensile strength (3.21MPa) and flexural strength (5.42MPa) were also obtained at 10% replacement.
3. The density of the biochar hardened materials gradually reduced from 2521.0 kg/m³ with 25% biochar to 2348.2 kg/m³ with 40% biochar, a decrease of 6.85%. This reduction is only due to the lower specific gravity of biochar, which accounts for approximately 37% of the decrease.
4. The 10% replacement had the least 4.21% of water absorbed, then higher replacements resulted in more water absorption.
5. The carbonation depth showed an increase in depth with replacement up to 25% and then decreased at high dosage, from 3.2 mm to 15.1 mm.
6. More compact matrix is observed at low to intermediate doses and more porous regions are observed at high doses which are consistent with the observed trends as supported by SEM observations.
7. A replacement level of around 10% is a good fit to investigate, but is not a proven optimum value, until statistical analysis, durability testing conducted over a longer period and assessment against the M30 acceptance criteria are completed. At this level carbonation depth was about twice that of the control.
8. The results are based on three samples from each mixture and one source of biochar. Before the trends are considered to be significant, differences among mixtures should be confirmed using ANOVA with post hoc tests on the specimen-level data.

5. Limitations and Future Work

The study employed one type of biochar and one accelerated-carbonation condition and results cannot be extrapolated beyond the specific biochar mix design used. The following future work is suggested: Specimen-level statistics (including replicate variation); Biochar characterisation (particle size, XRD, EDS, TGA); Long-term natural carbonation; Reinforcement corrosion assessment at 5–10% replacement; and a verified life cycle assessment prior to claiming net carbon-emission reductions.

Declarations

Conflicts of interest:

No Conflict

Funding:

“This research received no external funding.

Author Contribution

MURUGESH INVESTIGATE THE TEST RESULTS, MANUSCRIPT FORMULATION. LEENA FORMULATE THE DATAS INJOURNAL

Acknowledgements:

Jct college of Engineering and Technology

Data availability:

availability of the raw test data

References

1. Andrew, R. M. (2018). Global CO_2 emissions from cement production. Earth System Science Data, 10, 195–217. https://doi.org/10.5194/essd-10-195-2018
2. Scrivener, K. L., John, V. M., Gartner, E. M. (2018). Eco-efficient cements: Potential economically viable solutions for a low-CO_2 cement-based materials industry. Cement and Concrete Research, 114, 2–26. https://doi.org/10.1016/j.cemconres.2018.03.015
3. ASTM C496/C496M. Standard Test Method for Splitting Tensile Strength of Cylindrical Concrete Specimens.
4. ASTM C78/C78M. Standard Test Method for Flexural Strength of Concrete (Using Simple Beam with Third-Point Loading).
5. ASTM C642. Standard Test Method for Density, Absorption, and Voids in Hardened Concrete.
6. Bureau of Indian Standards. IS 516: Methods of Tests for Strength of Concrete.
7. Bureau of Indian Standards. IS 12269:2013. Ordinary Portland Cement, 53 Grade – Specification.
8. RILEM CPC-18. Measurement of hardened concrete carbonation depth. Materials and Structures, 1988.

Figures

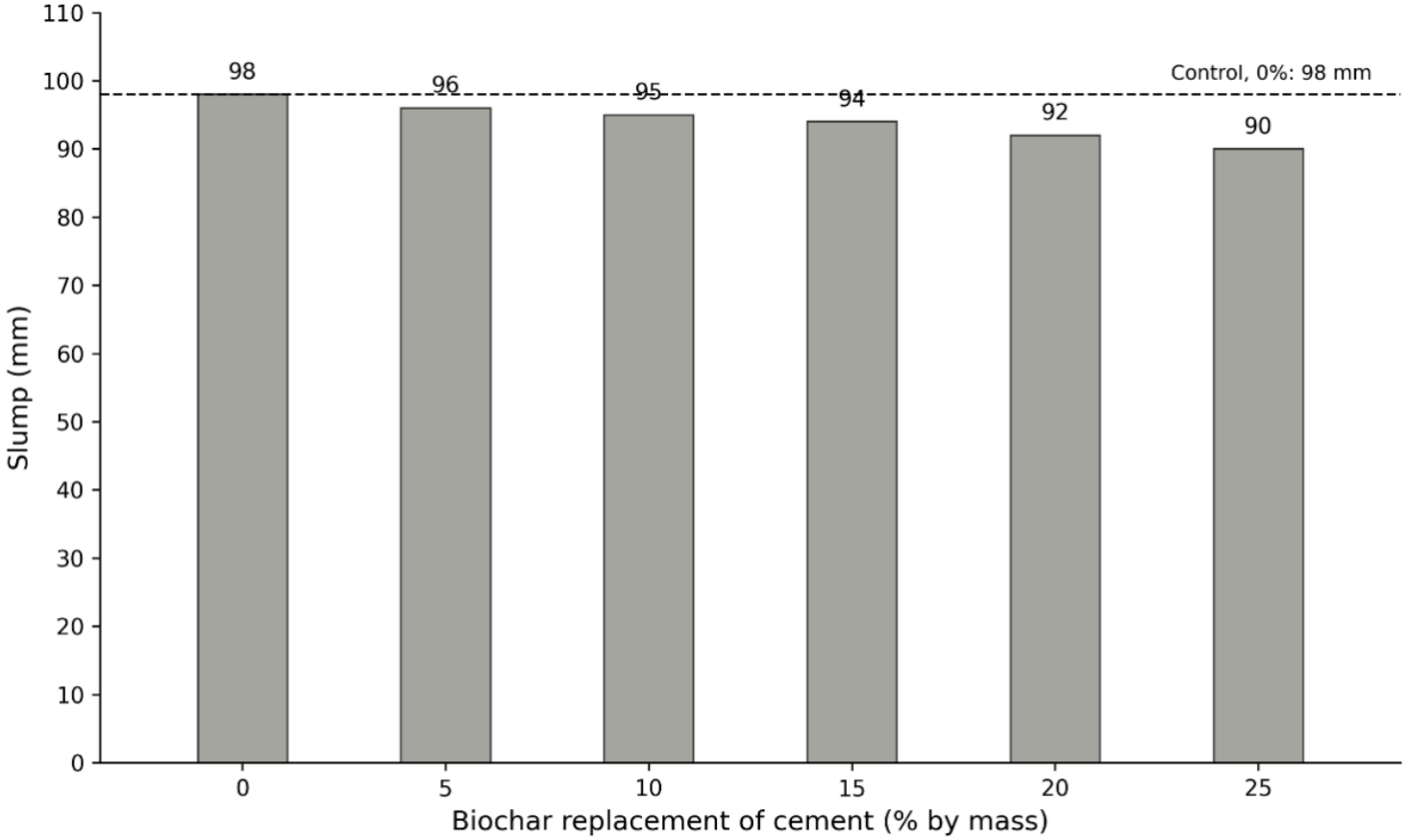


Figure 1

Fig. 1. Slump of the concrete mixtures at different biochar replacement levels.

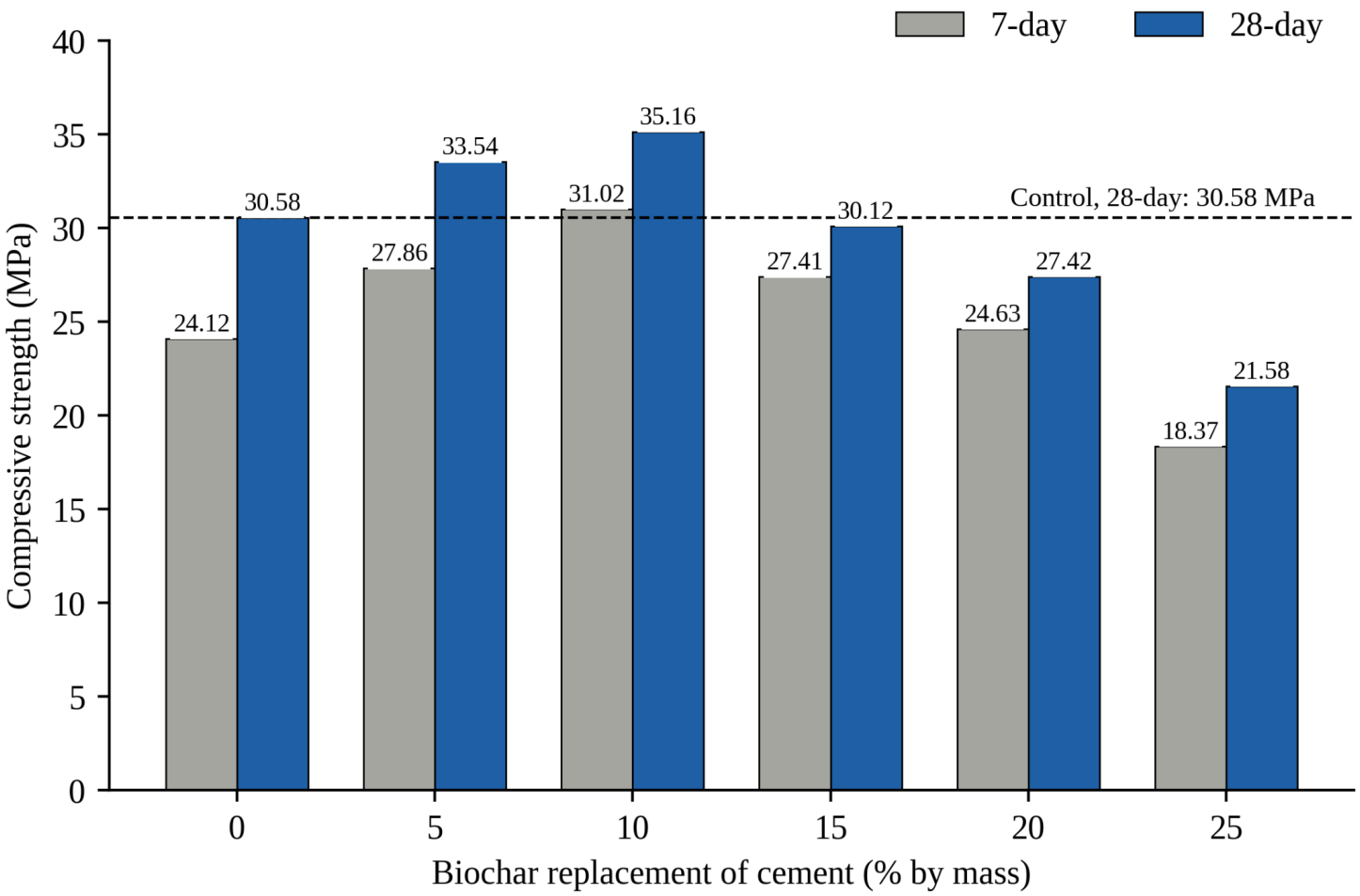


Figure 2

Fig. 2. Compressive strength of the six mixtures at 7 and 28 days (mean values).

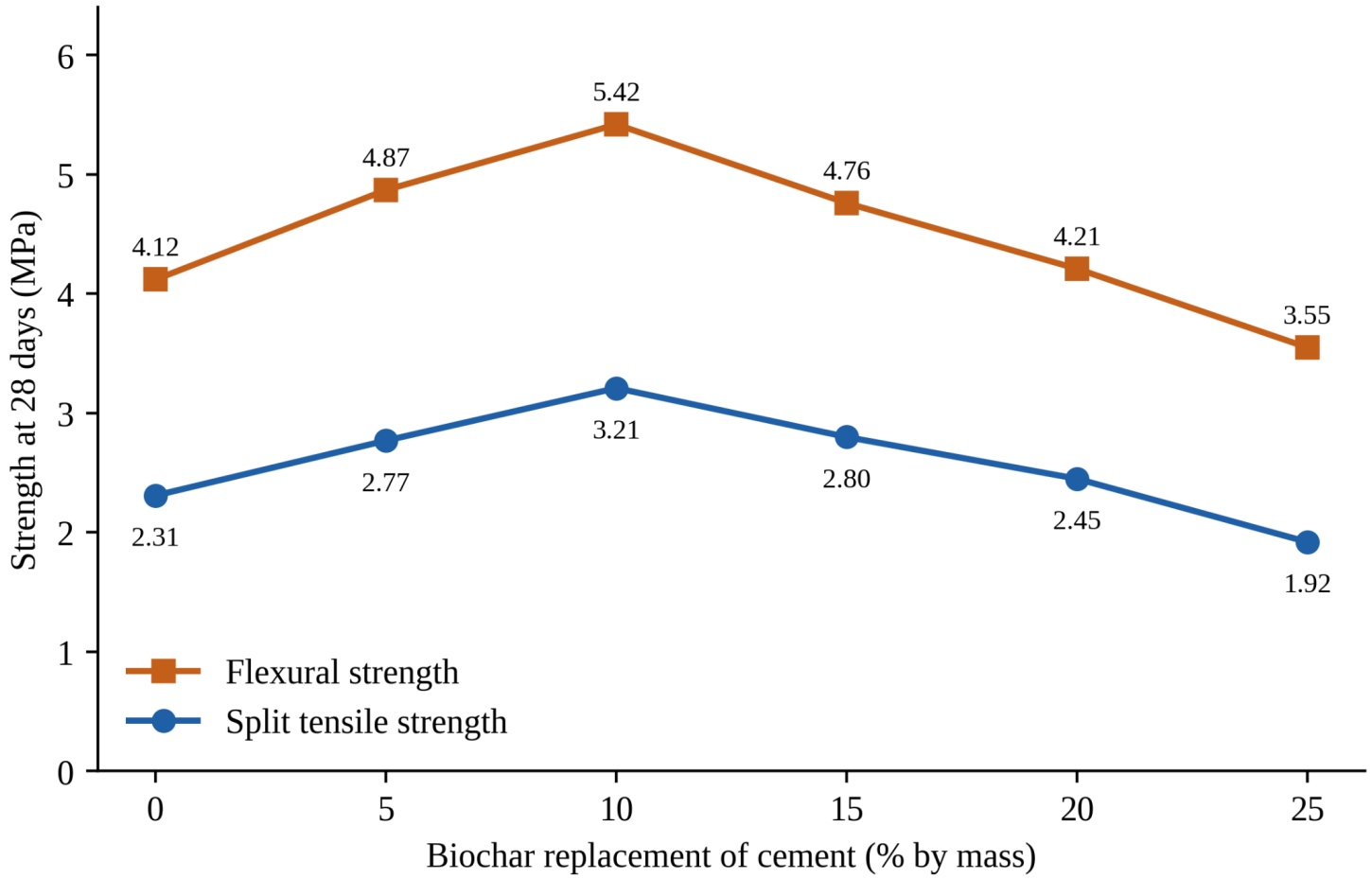


Figure 3

Fig. 3. Split tensile and flexural strength at 28 days versus biochar replacement level (mean values).

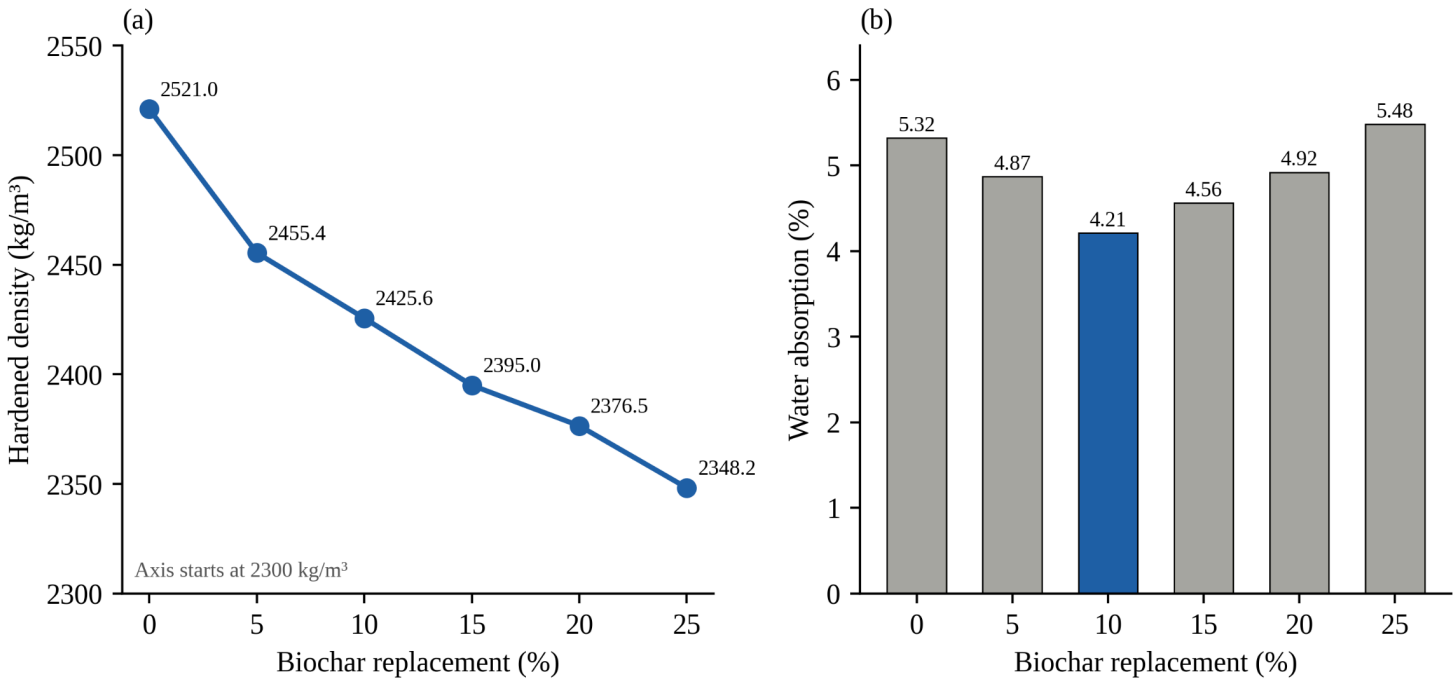


Figure 4

Fig. 4. Effect of biochar replacement on (a) hardened density and (b) water absorption at 28 days (mean values). The density axis starts at 2300 kg/m³.

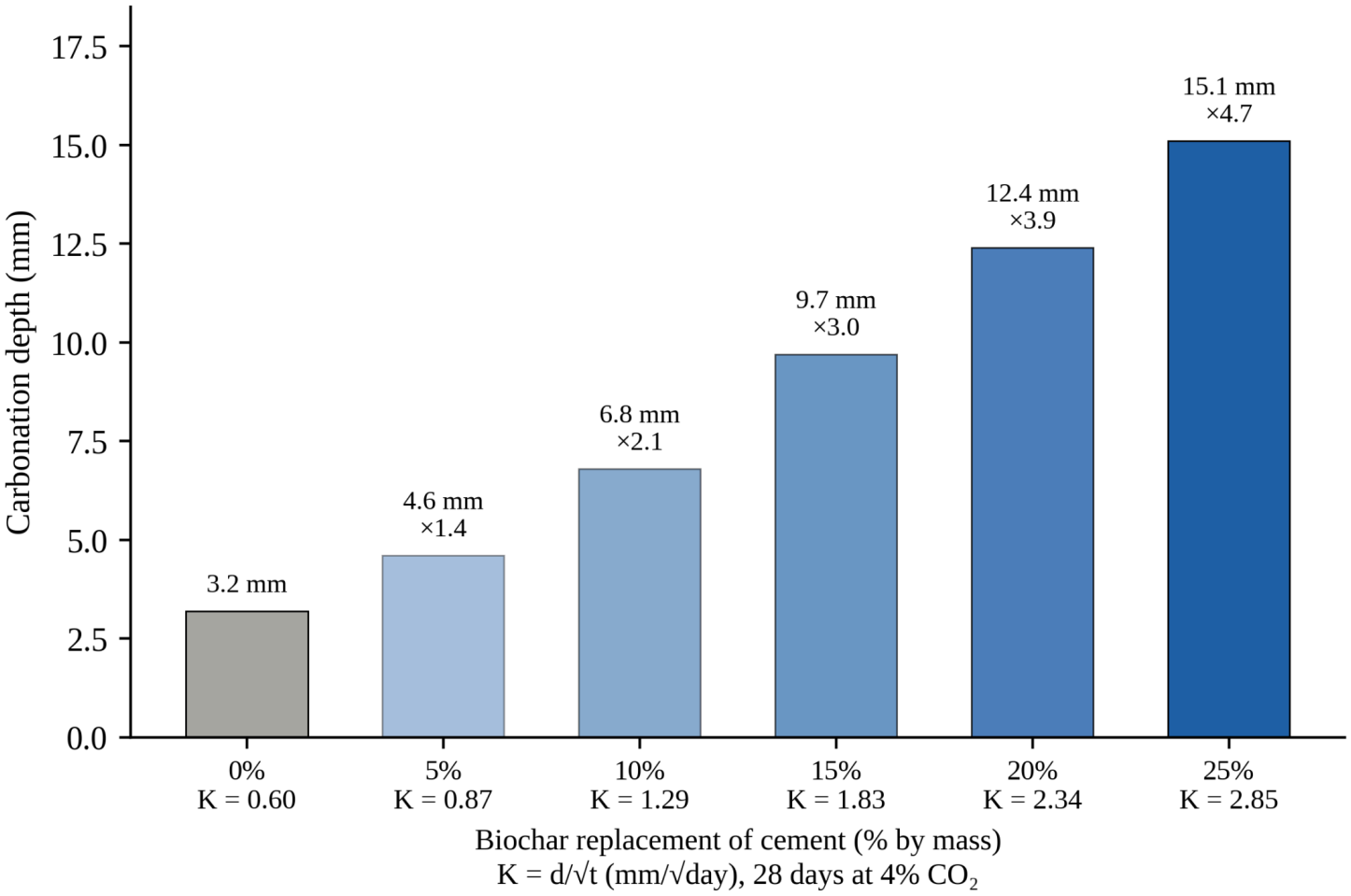


Figure 5

Fig. 5. Carbonation depth after 28 days of accelerated exposure (4% CO_2), with the ratio to the control and the apparent carbonation coefficient K = d/√t (mm/√day) for each mixture.

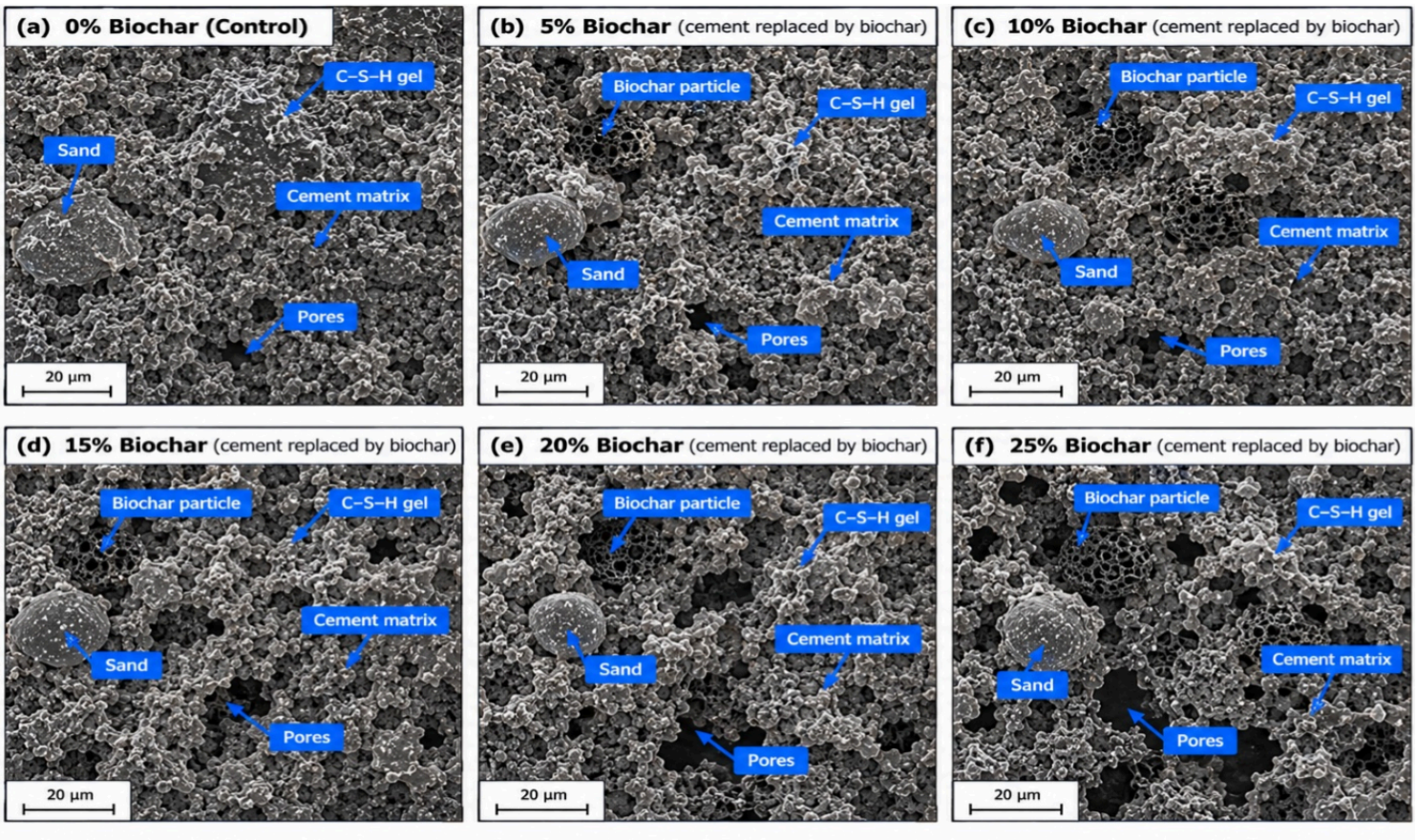


Figure 6

Fig. 6. SEM micrographs of concrete with (a) 0% (control), (b) 5%, (c) 10%, (d) 15%, (e) 20% and (f) 25% biochar replacement of cement.

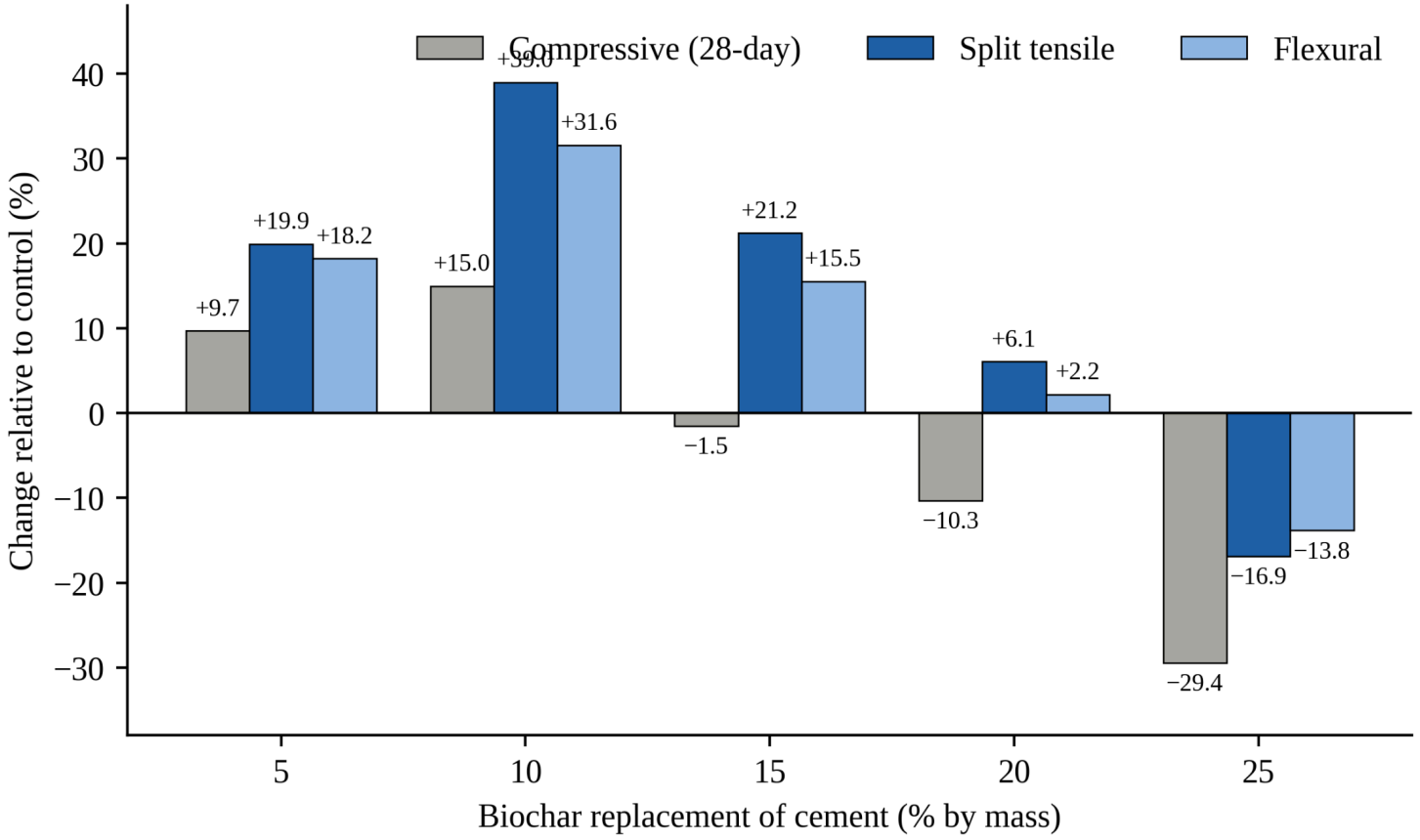


Figure 7

Fig. 7. Change in 28-day compressive, split tensile and flexural strength relative to the control, calculated from the mean values in Tables 11–13.